

Noisy Computations during Inference: Harmful or Helpful?

Minghai Qin*, Dejan Vucinic

Abstract

We study two aspects of noisy computations during inference. The first aspect is how to mitigate their side effects for naturally trained deep learning systems. One of the motivations for looking into this problem is to reduce the high power cost of conventional computing of neural networks through the use of analog neuromorphic circuits. Traditional GPU/CPU-centered deep learning architectures exhibit bottlenecks in power-restricted applications (e.g., embedded systems). The use of specialized neuromorphic circuits, where analog signals passed through memory-cell arrays are sensed to accomplish matrix-vector multiplications, promises large power savings and speed gains but brings with it the problems of limited precision of computations and unavoidable analog noise. We manage to improve inference accuracy from 21.1% to 99.5% for MNIST images, from 29.9% to 89.1% for CIFAR10, and from 15.5% to 89.6% for MNIST stroke sequences with the presence of strong noise (with signal-to-noise power ratio being 0 dB) by noise-injected training and a voting method. This observation promises neural networks that are insensitive to inference noise, which reduces the quality requirements on neuromorphic circuits and is crucial for their practical usage.

The second aspect is how to utilize the noisy inference as a defensive architecture against black-box adversarial attacks. During inference, by injecting proper noise to signals in the neural networks, the robustness of adversarially-trained neural networks against black-box attacks has been further enhanced by 0.5% and 1.13% for two adversarially trained models for MNIST and CIFAR10, respectively.

Keywords: deep learning, noisy inference, adversarial attacks

1. Introduction

Neural networks (NNs) [1, 2] are layered computational networks that try to imitate the function of neurons in a human brain during object recognition, decision making, and other cognitive tasks. They are one of the most widely used machine learning techniques due to their good performance in practice. Certain variants of neural networks were shown to be more suitable for different learning applications. For instance, deep convolutional neural networks (CNNs) [3, 4] were found to be effective at recognizing and classifying images.

*I am corresponding author

Email address: qinminghai@gmail.com (Minghai Qin)

Recurrent neural networks (RNNs) [5, 6] provide stronger performance at sequence predictions, e.g. speech or text recognition. A neural network is determined by the connections between the neurons and weights/biases associated with them which are trained using the back-propagation algorithm [7, 8].

In order to fit highly non-linear functions and thus to achieve a high rate of correctness in practice, neural networks usually contain many layers, each containing a large number of weights. The most power- and time-consuming computation of a neural networks is the matrix-vector multiplication between weights and incoming signals. In power-restricted applications, such as an inference engine in an embedded system, the size of the neural networks is effectively limited by the power consumption of the computations. One attractive method of lowering this power consumption is by use of neuromorphic computing [9], where analog signals passed through memory-cell arrays are sensed to accomplish matrix-vector multiplications. Here weights are programmed as conductances (reciprocal of resistivity) of memory cells in a two-dimensional array, such as resistive RAM (ReRAM), phase-change RAM (PCM) or NAND Flash [10]. According to Ohm’s law, if input signals are presented as voltages to this layer of memory cells, the output current is the matrix-vector multiplication of the weights and the input signals. The massive parallelism of this operation also promises significant savings in latency over sequential digital computations.

One of the problems with neuromorphic computing is the limited precision of the computations, since the programming of memory cells, as well as the measurement of the analog outputs, inevitably suffers from analog noise, which affects performance of deep learning systems in a harmful way. Some researchers have proposed to correct the errors between A/D and D/A converters of each layer [11, 12], which induces extra overhead in latency, space, and power as well. Existing noisy inference literature for neuromorphic computing is mostly in the device/circuit domain, typically focusing on redesigning memory devices/circuits to reduce the noise power. But to our knowledge, the exploration of robustness of neural networks against analog and noisy computations inside the network in an algorithmic point of view has not been studied in detail. It is the first goal of this paper to present methods and observations to mitigate the harmful effects brought by inference noise.

During its study, we find out that noisy inference can also be helpful to defend against black-box adversarial attacks of neural networks, the resistance of which is becoming more crucial for a wide range of applications, such as deep learning systems deployed in financial institutions and autonomous driving. Adversarial attacks manipulate inputs to a neural networks and generate adversarial examples that have rarely perceptible differences to a natural image, but they lead to incorrect predictions [13]. White-box attacks can be categorized into three categories.

- Single step attack, e.g., fast gradient sign methods (FGSM) [14],

$$x^* = x + \epsilon \cdot \text{sign}(\nabla_x J(x, y)),$$

where x and x^* is the natural and adversarial examples, respectively. ϵ is the upper bound on the L_∞ distance between x and x^* . $J(x, y)$ is the loss function for an input x being predicted to have label y and ∇_x is the derivative operator with respect to input x .

- Iterative methods, e.g., iterative FGSM [15],

$$x_0^* = x, x_{t+1}^* = \text{Clip}_{x,\epsilon}(x_t^* + \alpha \cdot \text{sign}(\nabla_x J(x_t^*, y))),$$

where α is the learning rate of the adversary, $\text{Clip}_{x,\epsilon}(\cdot)$ is a function that clips the output to be within the ϵ -cube of x such that the L_∞ distance between x_t^* and x is always less than or equal to ϵ .

- Optimization based attacks, e.g., [16],

$$\arg \min_{x^*} \lambda \|x - x^*\|_p + J(x^*, y),$$

where λ balances the L_p norm distortion and the loss function.

Black-box attacks are possible based on the transferability [17] of adversary such that adversarial examples generated from one neural network often lead to incorrect predictions of another independently trained neural network.

Several defensive mechanisms such as distillations [18], feature squeezing [19], and adversary detection [20], are proposed against attacks. [21] models the process as a min-max problem and builds a universal framework for attacking and defensive schemes, where it tries to provide a guaranteed performance for the first-order attacks, i.e., attacks based solely on derivatives. They also suggested that adversarial training with projected gradient descent (PGD) provides a strongest robustness against first-order attacks. Based on their study, we further investigate noisy inference of adversarially trained neural networks. Experimental results show improvement on robustness against black-box adversarial attacks and indicate that adversarial examples are more sensitive to inference noise than natural examples.

The contribution of this paper is summarized as follows.

1. We model the analog noise of neuromorphic circuits as additive and multiplicative Gaussian noise. The impact on accuracy of noisy inference is shown to be severe by three neural network architectures (a regular CNN, a DenseNet [22], and a LSTM-based RNN) for three datasets (MNIST, CIFAR10, and MNIST stroke sequences [23]), e.g., when noise power equals the signal power, the accuracy is as low as (21.1%, 29.9%, 10.1%), respectively.

2. We observe that the performance of noisy inference can be greatly improved by injecting noises to all layers in the neural networks during training. Noise-injected training was used as a regularization tool for better model generalization, but its application to noisy inference has not been studied in details. We provide a quantitative measurement on the impact that the inference noise has on noiseless-trained and noise-injected trained neural networks, where the power of training and inference noise might not match. The performance of noisy inference with low-to-medium noise power is improved to almost as good as noiseless inference. For large noise power (equal to signal power), the accuracy is increased to (77.7%, 66.9%, 66.9%) for the three datasets, respectively.

3. We further improve the performance of noisy inference by proposing a voting mechanism for large noise power. The accuracy has been further increased to (99.5%, 89.1%, 89.6%) for the three datasets when noise power equals the signal power. In addition, we observe that

with noise-injected training and the proposed voting mechanism combined, noisy inference can give higher accuracy (0.5%) than noiseless inference for LSTM-based recurrent neural networks, which is counterintuitive since it is often believed that noise during inference would be harmful rather than helpful to the accuracy.

4. A further study on adversarially trained neural networks for MNIST and CIFAR10 has shown that noisy inference improves the robustness of deep neural networks against black-box attacks. The accuracy of adversarial examples has been improved by 0.5% and 1.13% (in absolute values) for MNIST and CIFAR10 when validated on a separately and adversarially trained CNN and DenseNet, respectively.

2. Preliminaries

A neural network contains input neurons, hidden neurons, and output neurons. It can be viewed as a function $f : \mathcal{X} \rightarrow \mathcal{Y}$ where the input $x \in \mathcal{X} \subseteq \mathcal{R}^n$ is an n -dimensional vector and the output $y \in \mathcal{Y} \subseteq \mathcal{R}^m$ is an m -dimensional vector. In this paper, we focus on classification problems where the output $y = (y_1, \dots, y_m)$ is usually normalized such that $\sum_{i=1}^m y_i = 1$ and y_i can be viewed as the probability for some input x to be categorized as the i -th class. The normalization is often done by the softmax function that maps an arbitrary m -dimensional vector \hat{y} into normalized y , denoted by $y = \text{softmax}(\hat{y})$, as $y_i = \frac{\exp(\hat{y}_i)}{\sum_{i=1}^m \exp(\hat{y}_i)}$, $i = 1, \dots, m$. For top- k decision problems, we return the top k categories with the largest output y_i . In particular for hard decision problems where $k = 1$, the classification results is then $\arg \max_i y_i, i = 1, \dots, m$.

A feed-forward neural network f that contains n layers (excluding the softmax output layer) can be expressed as a concatenation of n functions $f_i, i = 1, 2, \dots, n$ such that $f = f_n(f_{n-1}(\dots f_1(x) \dots))$. The i th layer $f_i : \mathcal{X}_i \rightarrow \mathcal{Y}_i$ satisfies $\mathcal{Y}_i \subseteq \mathcal{X}_{i+1}$, $\mathcal{X}_1 = \mathcal{X}$. The output of last layer \mathcal{Y}_n is then fed into the softmax function. The function f_i is usually defined as

$$f_i(x) = g(W \cdot x + b), \quad (1)$$

where W is the weights matrix, b is the bias vector, and $g(\cdot)$ is an element-wise activation function that is usually nonlinear, e.g., tanh, sigmoid, rectified linear unit (ReLU) [24] and leaky ReLU [25]. Both W and b are trainable parameters.

In this paper, two noise models are assumed, which are additive Gaussian noise model $z \sim \mathcal{N}(0, \sigma^2)$ and multiplicative Gaussian noise model $z \sim \mathcal{N}(1, \sigma^2)$, respectively, in the forward pass after each matrix-vector multiplication. Then Eq. (1) becomes

$$f_i(x) = g(W \cdot x + b + z), \quad (2)$$

for additive Gaussian noise or

$$f_i(x) = g((W \cdot x + b) \cdot z) \quad (3)$$

for multiplicative Gaussian noise. Additive Gaussian noise $z \sim \mathcal{N}(0, \sigma^2)$ models procedures of neuromorphic computing where the noise power is irrelevant to the signals, such as signal

sensing, memory reading, and some random electrical perturbation of circuits. On the other hand for multiplicative noises, we can show that multiplying a unit-mean Gaussian random variable Z to a signal X is equivalent to adding a zero-mean Gaussian random variable Z' to the signal where the standard deviation of Z' is proportional to the magnitude of the signal, as

$$XZ = X(1 + Z') = X + XZ', \quad (4)$$

where $XZ' \sim \mathcal{N}(0, \sigma^2 X^2) = \mathcal{N}(0, (|X|\sigma)^2)$. Therefore, multiplicative noise models the procedures where the noise power is proportional to the signal power, such as memory programming and computations.

For both additive and multiplicative Gaussian noise models, we denote σ_{train} and σ_{val} the standard deviation of the noise during training and validation (inference), respectively. We denote $\sigma_{\text{train},+}$, $\sigma_{\text{val},+}$, $\sigma_{\text{train},\times}$, $\sigma_{\text{val},\times}$ if specific additive or multiplicative noise models are referred to. Note that σ_{train} is usually set to be 0 in conventional training; Nonetheless, random noise is sometimes injected ($\sigma_{\text{train}} > 0$) during training to provide better generalization. Conventional deep learning architecture assumes $\sigma_{\text{val}} = 0$ since digital circuits are assumed to have no errors during computations.

For both noisy models, the signal-to-noise power ratio (SNR) is a defining parameter that measures the strength of the noise relative to the signal, which is defined as the ratio between the power of signal and noise. It is usually expressed in dB where $\text{SNR}(\text{dB}) = 10 \log_{10}(\text{SNR}(\text{value}))$. For example, if the signal and noise has the same power, $\text{SNR} = 1$ (or 0 dB). For multiplicative noise models, we have constant $\text{SNR} = \frac{1}{\sigma_{\text{val},\times}^2}$; on the other hand, SNRs for additive noise models with fixed $\sigma_{\text{val},+}$'s depend highly on signal power and it would be a fair comparison only if the signal power is invariant. Therefore, we mainly use multiplicative noise models in our experiment except for the case where we can normalize the signals to have constant power.

3. Robustness of NNs against Noisy Inference

In this section we explore the robustness of neural networks against noisy computations modeled in Eq. (2) and Eq. (3). We will show the robustness of different neural network architectures for different datasets against noisy inference and provide two techniques that improve the robustness, namely, noise-injected training and voting.

3.1. Datasets and NN architectures

Three datasets are used in our experiments, which are MNIST images (60000 for training and 10000 for validation), CIFAR10 images (50000 for training, 10000 for validation, no data augmentation applied), and the stroke sequence of MNIST [23] for each MNIST image.

For MNIST images, we use a 6-layer convolutional neural network described in Table 1. The noiseless trained model has prediction accuracy of 99.5% for noiseless inference. For multiplicative Gaussian noise models, the parameters in batch normalization layers are trainable. However, for additive Gaussian noise models, we use batch normalization layers with

Table 1: A 6-layer CNN architecture for MNIST

Layer	Output shape
Conv. 2D (3, 3) - Batch Norm (β, γ)	(26, 26, 32)
Gaussian Noise - ReLu	(26, 26, 32)
Conv. 2D (3, 3) - Batch Norm (β, γ)	(24, 24, 32)
Gaussian Noise - ReLu	(24, 24, 32)
Maxpooling	(12, 12, 32)
Conv. 2D (3, 3) - Batch Norm (β, γ)	(10, 10, 64)
Gaussian Noise - ReLu	(10, 10, 64)
Conv. 2D (3, 3) - Batch Norm (β, γ)	(8, 8, 64)
Gaussian Noise - ReLu	(8, 8, 64)
Maxpooling	(4, 4, 64)
Fully connected - Batch Norm (β, γ)	(256)
Gaussian Noise - ReLu	(256)
Fully connected - Gaussian Noise	(10)

fixed parameters $\beta = 0, \gamma = 1$ (as opposed to trainable mean and variance) to minimize the signal power variations for the reason mentioned in Section 2.

For CIFAR10, we use a densely connected convolutional neural network (DenseNet) [22]. DenseNet is an enhanced version of ResNet [26] where all feature maps of previous layers are presented as the input to later convolutional layers. The depth of the DenseNet is 40 and growth rate is 12. All parameters in convolutional, fully-connected and batch normalization layers are trainable since fixed batch normalization parameters cannot provide satisfactory accuracy even if the inference is noiseless. The total number of trainable parameters of the DenseNet is around one million. The noiseless trained model has prediction accuracy of 92.5% with noiseless inference, which is slightly below the reported value (93%) in [26]. We inject multiplicative Gaussian noise after each matrix-vector multiplication.

For MNIST stroke sequences extracted by [23], we use a LSTM-based recurrent neural network with 50 cells corresponding to the first 50 two dimensional coordinates of pen-points of each written digit. If the total number of pen-points is less than 50, it is padded with (0, 0)'s. Since the pen-points are two dimensional, the input dimension to each LSTM cell is 2. The number of hidden units in each cell is 128, and the last LSTM cell are connected with an output layer of 10 neurons for classification. The noiselessly trained model has accuracy around 95% with noiseless inference. The drop of accuracy from MNIST images to MNIST stroke sequences may due to that we have to truncate or pad pen-points to fit the 50 LSTM cells and gray level information is lost when converting images to stroke sequences. There are four matrix-vector multiplications in each LSTM cell (see four yellow boxes in LSTM cells in Fig. 1) and one between the LSTM cell and the output layer, where multiplicative noise are injected.

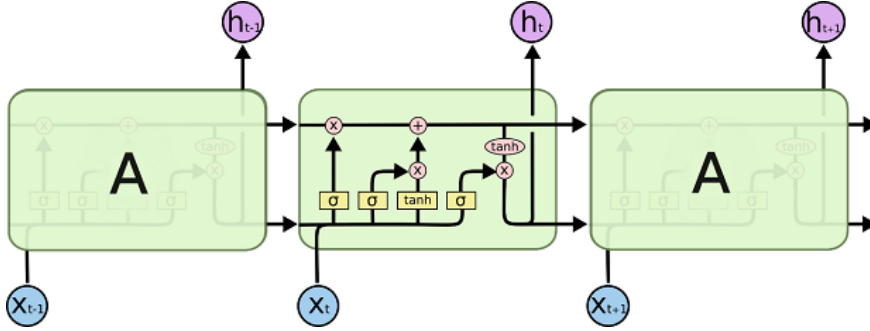


Figure 1: Example of LSTM cells.

3.2. Noisy Inference by Noiseless and Noise-Injected Training

In this section, we show the impact of noisy inference on accuracy for noiselessly and noise-injected trained models. The noise-injected training applies noise layers during training and thus the information in the forward pass is changed and consequently influences the weight updates during backward pass. We train models with different σ_{train} 's and use different σ_{val} 's to test the accuracy on all trained models. That is, the noise power in training does not necessarily match the noise power during inference. We will show that such noise-injected training uniformly improves accuracy on all σ_{val} 's.

3.2.1. The CNN for MNIST images

For MNIST images with the 6-layer CNN architecture, we train 100 epochs using stochastic mini-batch training with Adam optimizer and batch size being 32 for each $\sigma_{\text{train}} = 0.0$ to 1.0 with a step size of 0.1. The accuracy of noiselessly trained model ($\sigma_{\text{train}} = 0$) with noiseless inference ($\sigma_{\text{val}} = 0$) is around 99.5%. Then the 11 trained models are tested on validation set with $\sigma_{\text{val}} = 0.0$ to 1.0 with a step size of 0.1. We present the results of a subset of σ_{train} 's in Figure 2. Validation accuracy for each $(\sigma_{\text{train}}, \sigma_{\text{val}})$ pair is the average of 50 independent runs and we observe that all 50 results are highly concentrated in their average (within less than 1% variation). This phenomenon is also confirmed from neural network models for other datasets, thus we use the average accuracy as a measurement of robustness against noisy inference. Also note that y -axis represents the error rate ($1 - \text{accuracy}$) in logarithm scale. Table 2 and Table 3 summarize the results. The first row is the inference noise levels from $\sigma_{\text{val}} = 0.0$ to 1.0 with a step size of 0.2; the second row shows the accuracy for noiselessly trained models; the third row shows the best accuracy for σ_{val} in that column, which is achieved by noise-injected training with σ_{train} in the fourth row.

Table 2: Accuracy of noisy inference for multiplicative noise models for MNIST images.

$\sigma_{\text{val}, \times}$	0.0	0.2	0.4	0.6	0.8	1.0
$\sigma_{\text{train}, \times} = 0$	99.5%	99.3%	93.5%	65.7%	38.8%	21.1%
Best accu.	99.6%	99.5%	99.3%	94.6%	86.1%	77.7%
By $\sigma_{\text{train}, \times}$	0.2	0.5	0.5	0.7	1.0	1.0

Table 3: Accuracy of noisy inference for additive noise models for MNIST images.

$\sigma_{\text{val},+}$	0.0	0.2	0.4	0.6	0.8	1.0
$\sigma_{\text{train},+}=0$	99.5%	99.3%	95.8%	80.5%	58.8%	38.7%
Best	99.6%	99.5%	99.4%	99.2%	99.0%	98.4%
By $\sigma_{\text{train},+}$	0.4	0.4	0.4	0.6	0.9	1.0

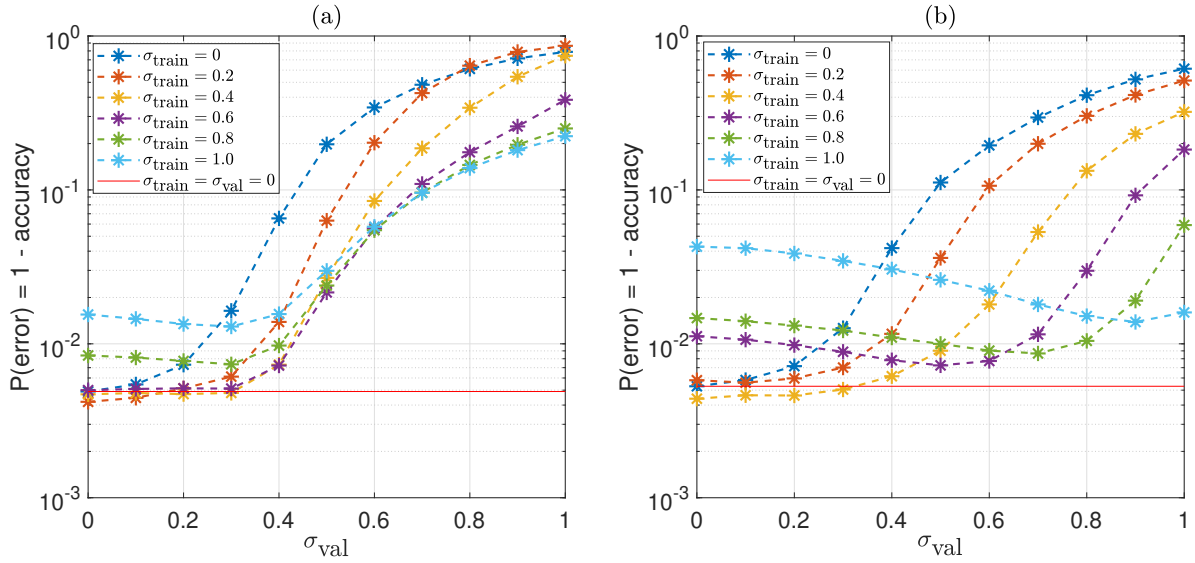


Figure 2: Validation accuracy of the 6-layer CNN with Gaussian noise for different $(\sigma_{\text{train}}, \sigma_{\text{val}})$ pairs. (a) Multiplicative noise model. (b) Additive noise model.

There are some observations that we can make from Table 2, Table 3, and Figure 2.

1. Conventional noiseless training ($\sigma_{\text{train}} = 0$) does not provide satisfactory performance against noisy inference even when the noise power is from low to medium (second row in Table 2 and Table 3). For example, when $\sigma_{\text{val}} = 0.4$, the accuracy reduces by 5.8% and 3.6% for multiplicative and additive noise models, respectively.

2. If the inference noise power is known, training with properly injected noise can greatly improve noisy inference (third and fourth row in Table 2 and Table 3) when the noise power is from low to medium (e.g., accuracy decreases less than 0.2% when $\sigma_{\text{val},\times} \leq 0.4$ and less than 0.3% when $\sigma_{\text{val},+} \leq 0.6$). Note that $\sigma_{\text{val},\times}$ is the ratio between standard deviations of noise and magnitude of signals and tolerating $\sigma_{\text{val},\times} = 0.4$ (SNR = 7.96 dB) is already a good relaxation on the requirement for neuromorphic circuits.

3. If the inference noise power is unknown, noise-injected training with a specified σ_{train} also provides consistent accuracy improvement for low-to-medium values of inference noise power (Figure 2). For example, the accuracy decreases less than 0.2% when $\sigma_{\text{train}} = 0.4$ for all inference noise level $\sigma_{\text{val}} \leq 0.4$ in both multiplicative and additive noise models.

We further investigate the learning speed and the weights of noise injected training. The result for multiplicative noise models is presented in Figure 3, where the learning curve (validation accuracy and loss) for the first 25000 stochastic mini-batches of size 32 is shown. It can be observed that higher noise power in training generally results in a lower training speed (with learning rate is fixed to be 0.0001). Table 4 shows the expected L_2 norm of weights for 11 trained CNN models with different $\sigma_{\text{train},\times}$. It can be seen that the magnitude of weights for $\sigma_{\text{train},\times} > 0$ are similar and are slightly greater than noiselessly trained model.

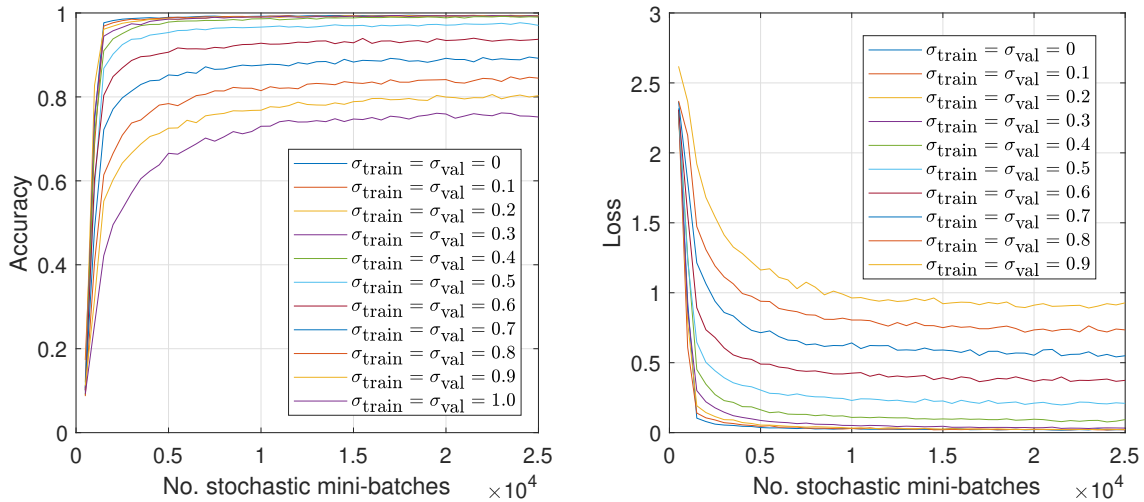


Figure 3: Learning curves of the noise injected training for $\sigma_{\text{train},\times} = 0.0$ to 1.0.

In order to understand the difference between models from noiseless and noise-injected training, we choose two 6-layer CNN models, corresponding to $\sigma_{\text{train},\times} = 0.0$ and 1.0, and run multiplicative noisy inference with $\sigma_{\text{val},\times} = 0.0$ to 1.0 for 10000 times for one same image

Table 4: Expected L_2 norm of all weights of 11 models

$\sigma_{\text{train},\times}$	0	0.1	0.2	0.3	0.4	0.5
$\sqrt{E(w^2)}$	0.049	0.054	0.054	0.059	0.060	0.060
$\sigma_{\text{train},\times}$	0.6	0.7	0.8	0.9	1.0	
$\sqrt{E(w^2)}$	0.058	0.056	0.060	0.058	0.059	

(which has label “6”) and then plot the distributions of 10 outputs after the softmax layers, which can be thought as the probability of that image being classified as the corresponding digits. Figure 4 and Figure 5 shows the evolution of the output distributions with increasing $\sigma_{\text{val},\times}$. Note that the upper right part in each of the six plots indicates higher probability of having large output values. Therefore, it is likely for the neural network to predict the image as labels/curves that appear in that area. It can be seen that noiselessly trained model (Figure 4) starts to be confused with digit “6” (pink) and “8” (dark yellow) when $\sigma_{\text{val},\times} \geq 0.6$; on the other hand, noise-injected training constantly favors the prediction of “6”.

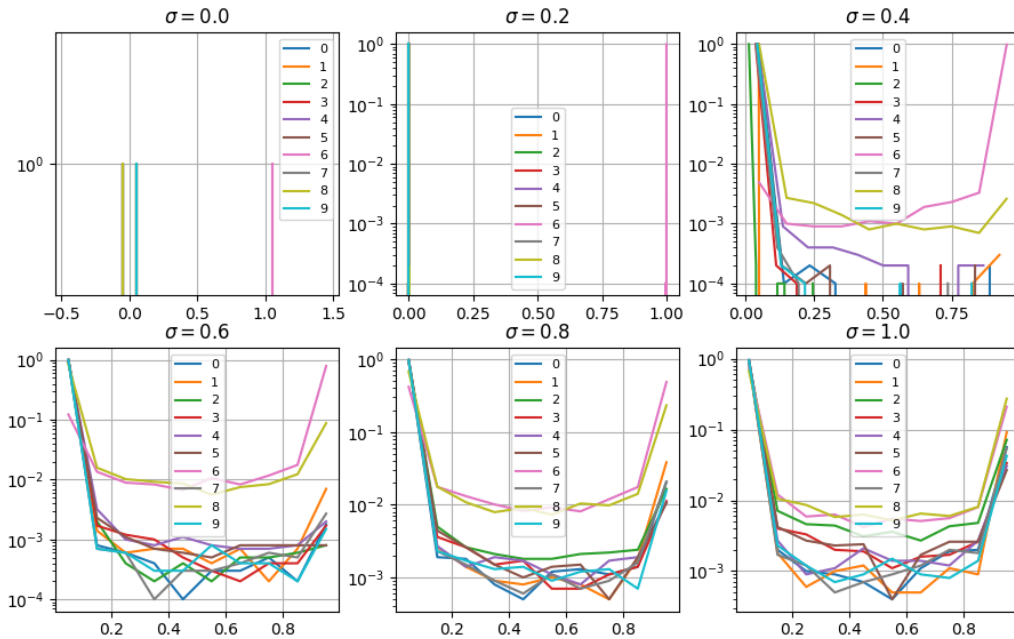


Figure 4: Distribution of the 10 softmax output for MNIST. Model based on conventional training at $\sigma_{\text{train},\times} = 0.0$, inference with validation noise $\sigma_{\text{val},\times} = 0$ to 1.0 at a step of 0.2.

3.2.2. A Depth-40 DenseNet for CIFAR10

We train the non-augmented dataset of CIFAR10 for 300 epochs using momentum optimizer with mini-batch of size 32. We inject multiplicative Gaussian noise right af-

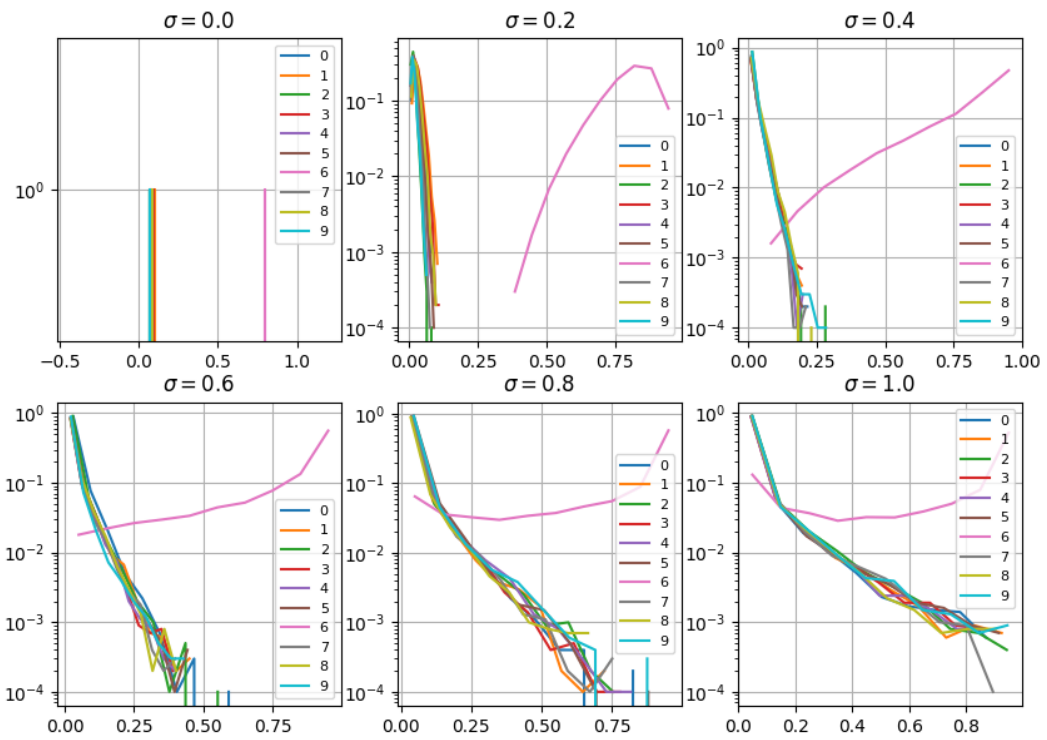


Figure 5: Distribution of the 10 softmax output for MNIST. Model based on noise-injected training at $\sigma_{\text{train},x} = 1.0$, inference with validation noise $\sigma_{\text{val},x} = 0$ to 1.0 at a step of 0.2 .

ter each matrix-vector multiplication. Figure 6 shows the average accuracy for pairs of $(\sigma_{\text{train},x}, \sigma_{\text{val},x})$, where Table 5 summarizes the results.

Similar to the 6-layer CNN for MNIST images, we can also conclude from Table 5 and Figure 6 for the multiplicative noise models that noise-injected training provides large robustness gain against noisy inference, e.g., accuracy decreases less than 1.3% (see Table 5) if $\sigma_{\text{val},x} \leq 0.4$ (SNR = 7.96 dB).

Table 5: Accuracy of noisy inference for multiplicative noise models for CIFAR10.

$\sigma_{\text{val},x}$	0.0	0.2	0.4	0.6	0.8	1.0
$\sigma_{\text{train},x}=0$	92.5%	91.9%	88.5%	78.7%	60.4%	29.9%
Best	92.8%	92.4%	91.5%	85.6%	75.7%	66.9%
By $\sigma_{\text{train},x}$	0.1	0.2	0.4	0.6	0.8	1.0

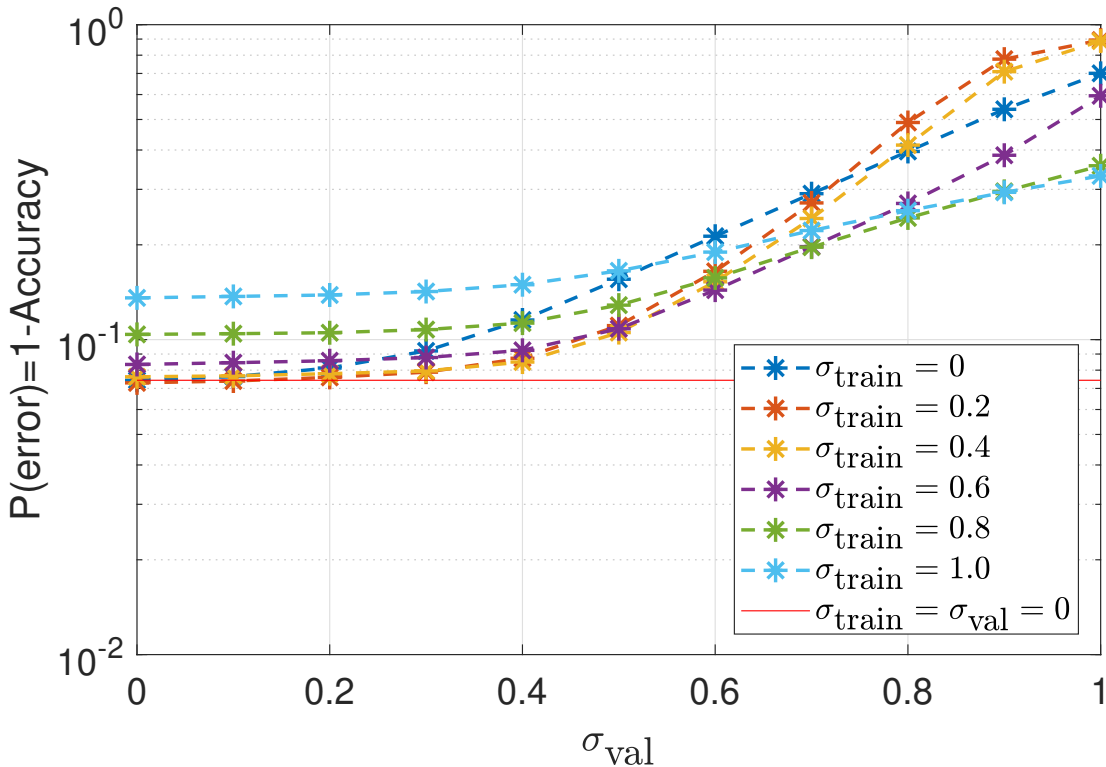


Figure 6: Validation accuracy of the depth-40 DenseNet with Gaussian noise for different $(\sigma_{\text{train},x}, \sigma_{\text{val},x})$ pairs.

3.2.3. LSTMs for MNIST stroke sequences

This section provides results on classifying stroke sequences on MNIST. We train LSTM-based RNNs for 100 epochs with stochastic mini-batch of batchsize 32 with Adam optimizer, where multiplicative noise are injected after four matrix-vector multiplications within the

LSTM cells and one for the final output layer. Figure 7 shows the accuracy for different $(\sigma_{\text{train},\times}, \sigma_{\text{val},\times})$ pairs and Table 6 summarizes the results. The accuracy for noise-injected training decreases less than 1.3% when $\sigma_{\text{val},\times} \leq 0.4$, providing much larger robustness than noiseless training against noisy inference.

Table 6: Accuracy of noisy inference for multiplicative noise models for MNIST stroke sequences.

$\sigma_{\text{val},\times}$	0.0	0.2	0.4	0.6	0.8	1.0
$\sigma_{\text{train},\times}=0$	94.8%	88.0%	49.8%	23.6%	17.0%	15.5%
Best accu.	95.6%	95.7%	94.3%	87.3%	77.0%	66.9%
By $\sigma_{\text{train},\times}$	0.3	0.3	0.4	0.6	0.8	1.0

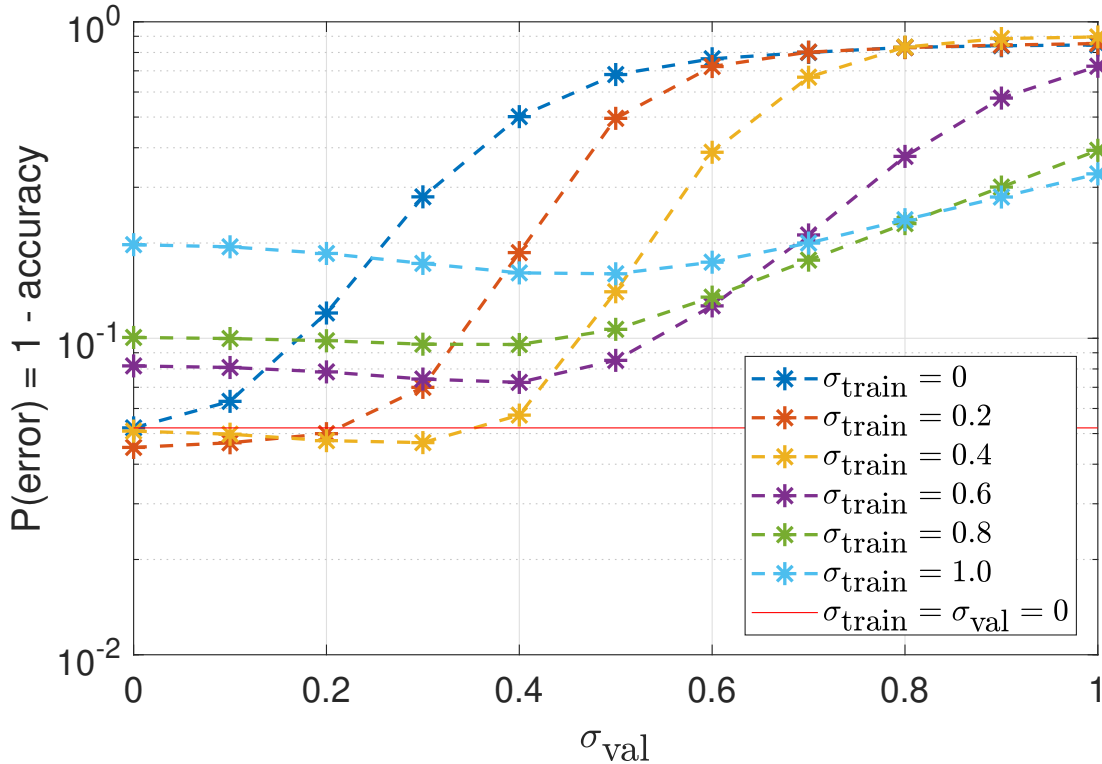


Figure 7: Validation accuracy of LSTM-based RNNs for different $(\sigma_{\text{train},\times}, \sigma_{\text{val},\times})$ pairs.

3.3. Noisy Inference with Voting

Inspired by the comparison of Figure 4 and Figure 5, we find many instances where the correct prediction is favored in the histogram however not correctly predicted when σ_{val} is large, e.g., 1.0. The reason is that the prediction is probabilistic, i.e., if there is a small overlap in the histogram, e.g., 10%, between the favored correct label and a wrong label, the accuracy will be reduced by around 10%. Observing that the correct prediction appears more often in multiple runs of independent noisy inference, we propose a voting mechanism that

can magnify the favored label based on Law of Large Numbers, where we collect a number of predictions of noisy inference and claim the prediction with the most votes (also known as the **mode**) as the final prediction. Figure 8, Figure 9, and Figure 10 show a detailed comparison for inference with voting (b) and without voting (a), where three (a) sub-figures are replots of Figure 2(a), Figure 6, and Figure 7 for comparing purposes. Table 7, Table 8, and Table 9 summarize the results, where the second row repeats the best accuracy for noise-injected training and the third row are the best accuracy achieved by 20 votes on noisy inference using neural network models trained with $\sigma_{\text{train},x}$ equal to the corresponding column in the fourth row.

We can make a few observations based on Figure 8, Figure 9, Figure 10, Table 7, Table 8, and Table 9.

1. While the accuracy in low-to-medium $\sigma_{\text{val},x}$ (i.e., high SNR) regime is similar, voting further improves the accuracy of all three neural networks for three datasets when the noise power is large ($\sigma_{\text{val},x}$ close to 1.0). For example, when $\sigma_{\text{val},x} = 1.0$ (SNR = 0 dB), accuracy is improved by more than 20%, from (77.7%, 66.9%, 66.9%) to (99.5%, 89.1%, 89.6%) for MNIST images, CIFAR10, and MNIST stroke sequences, respectively. Compared horizontally, accuracy maintains almost the same (99.6% vs 99.5%) for MNIST images when $\sigma_{\text{val},x} = 1.0$ (SNR=1 in value or 0 dB). Noise-injected training without voting has such high accuracy only when $\sigma_{\text{val},x} \leq 0.2$ (SNR=25 in value or 14 dB), where a 14 dB gain is realized by voting. Similarly, the tolerable $\sigma_{\text{val},x}$ increases from 0.4 to 0.8 (a 6 dB SNR gain) for DenseNet of CIFAR10 if 1.5% accuracy loss is acceptable; the tolerable $\sigma_{\text{val},x}$ increases from 0.4 to 0.6 (a 3.5 dB SNR gain) for LSTMs of MNIST stroke sequences if 1% accuracy loss is acceptable. Such SNR gains further relax the requirements for neuromorphic circuit designs and enable them to have competitive accuracy with GPU/CPU centered digital computations.

2. We observe in Table 6 that with voting and noise-injected training combined, noisy inference improves 0.5% accuracy upon noiseless inference for LSTM-based recurrent neural networks, which is counterintuitive since it is often believed that noise during inference would be harmful rather than helpful to the performance. The improvement by noisy inference is also confirmed by independently training multiple LSTM models.

Table 7: Accuracy of noisy inference by voting for multiplicative noise models for MNIST images.

$\sigma_{\text{val},x}$	0.0	0.2	0.4	0.6	0.8	1.0
No voting	99.6%	99.5%	99.3%	94.6%	86.1%	77.7%
Best voting	99.6%	99.6%	99.6%	99.6%	99.6%	99.5%
By $\sigma_{\text{train},x}$	0.2	0.5	0.5	0.5	0.8	0.9

Having observed the benefits of the voting mechanism, we then discuss how to mitigate their weakness in practical applications since latency and power consumption will be increased when a prediction is made by multiple runs of noisy inference. Fig. 11(a) and (b) shows the trade-offs between the number of votes and accuracy for MNIST images and CIFAR10, respectively. It can be seen that the accuracy improves fast when the number

Table 8: Accuracy of noisy inference by voting for multiplicative noise models for CIFAR10.

$\sigma_{\text{val}, \times}$	0.0	0.2	0.4	0.6	0.8	1.0
No voting	92.8%	92.4%	91.5%	85.6%	75.7%	66.9%
Best voting	92.8%	92.7%	92.7%	92.8%	91.3%	89.1%
By $\sigma_{\text{train}, \times}$	0.1	0.1	0.2	0.3	0.6	0.8

Table 9: Accuracy of noisy inference by voting for multiplicative noise models for MNIST stroke sequences.

$\sigma_{\text{val}, \times}$	0.0	0.2	0.4	0.6	0.8	1.0
No voting	95.6%	95.7%	94.3%	87.3%	77.0%	66.9%
Best voting	95.6%	96.1%	95.9%	94.6%	92.7%	89.6%
By $\sigma_{\text{train}, \times}$	0.3	0.3	0.4	0.6	0.7	0.8

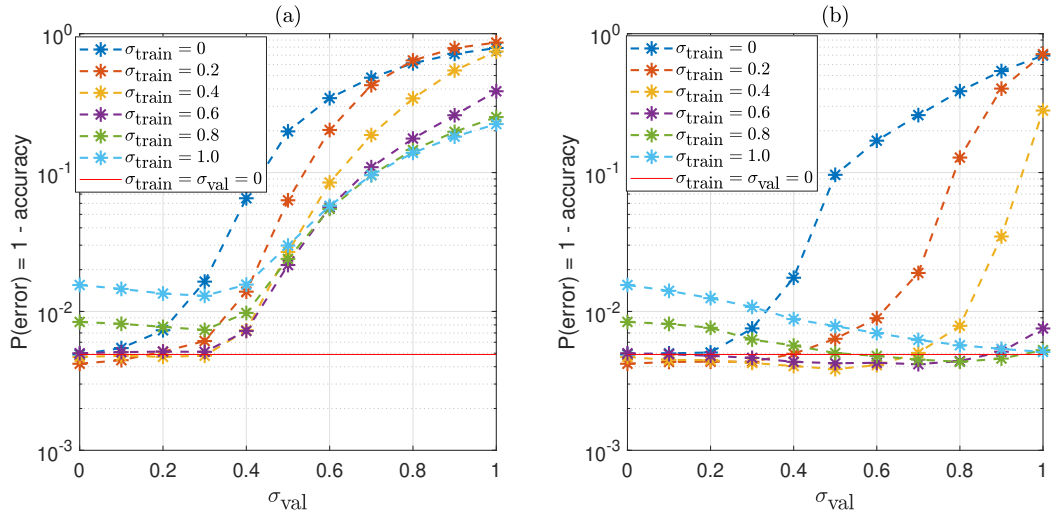


Figure 8: Validation accuracy of the 6-layer CNN for MNIST with multiplicative Gaussian noise of different $(\sigma_{\text{train}, \times}, \sigma_{\text{val}, \times})$ pairs. (a) One single inference. (b) Inference by voting with 20 runs.

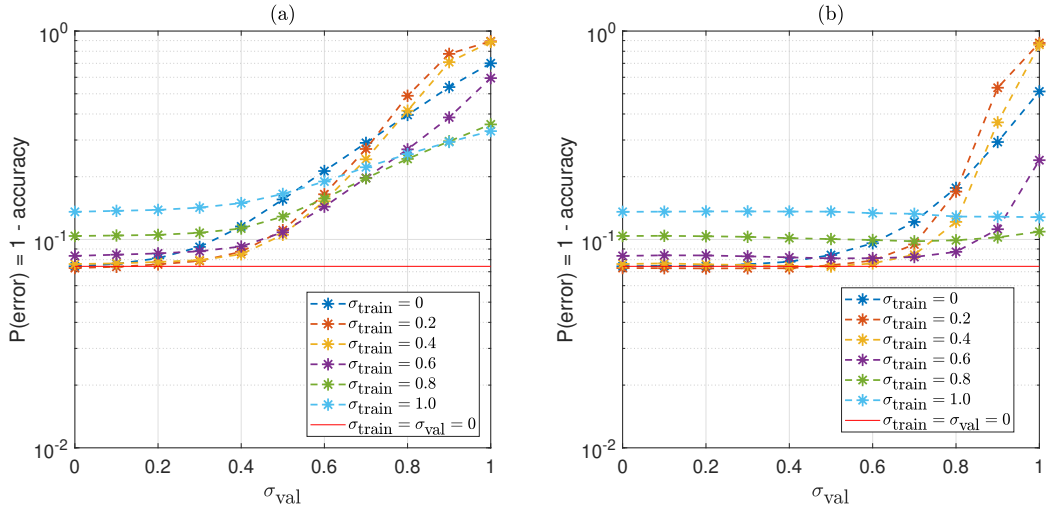


Figure 9: Validation accuracy of the depth-40 DenseNet for CIFAR10 with multiplicative Gaussian noise of different $(\sigma_{\text{train},x}, \sigma_{\text{val},x})$ pairs. (a) One single inference. (b) Inference by voting with 20 runs.

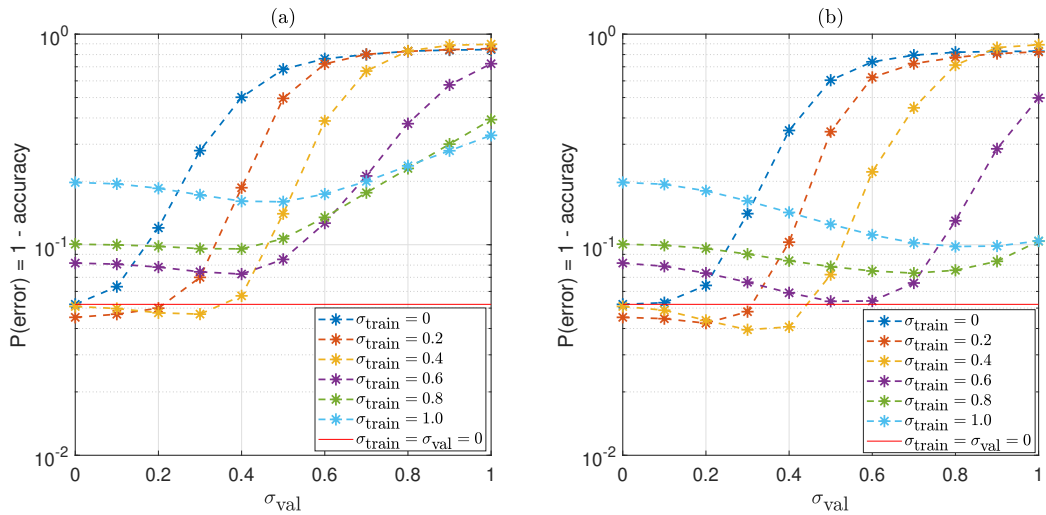


Figure 10: Validation accuracy of the LSTM-based RNN for MNIST stroke sequences with multiplicative Gaussian noise of different $(\sigma_{\text{train},x}, \sigma_{\text{val},x})$ pairs. (a) One single inference. (b) Inference by voting with 20 runs.

of votes increases from 1 to 10, in particular for large noise power. Beyond 10 votes, the accuracy curve becomes almost flat. Fast convergence of the voting is particularly critical for neuromorphic circuits-based deep neural networks to have smaller latency and power overhead.

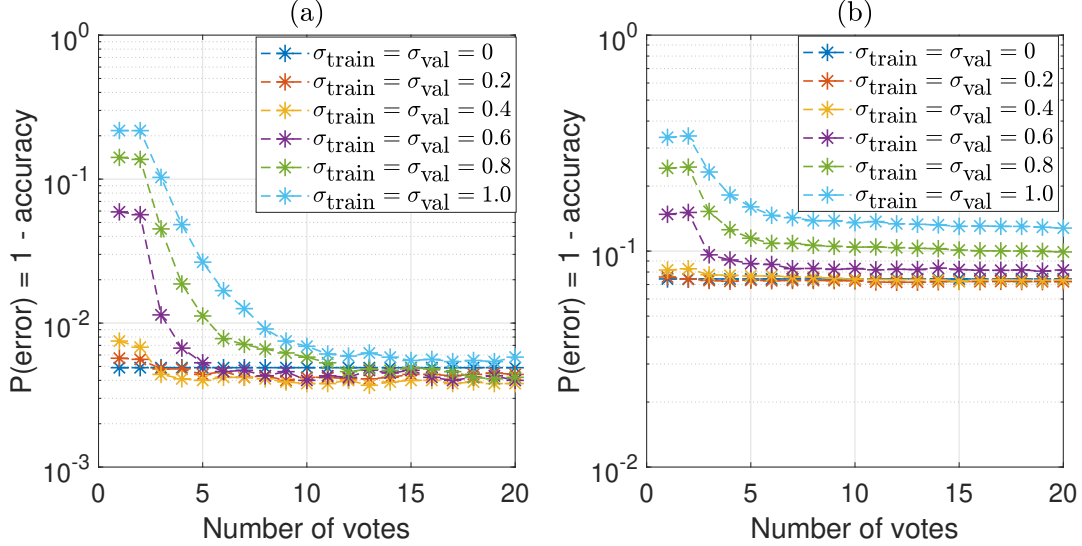


Figure 11: Trade-offs between number of votes and the accuracy of noisy inference for MNIST images (a) and CIFAR10 (b).

The latency overhead can be reduced in two ways. If the chip area is not a bottleneck, then multiple inference can be made in parallel from multiple copies of neuromorphic circuits-based neural networks, resulting in zero latency overhead. Otherwise, it can also be minimized by pipelining multiple inference on a single neuromorphic circuits-based neural network. Each layer of a neural network can be implemented as one memory array and instead of waiting for one inference to finish before the next one to start, images can be fed into the neuromorphic computing system at each time stamp and all layers form a pipeline. Assume the number of layers is L , each layer contributes latency T , and the number of votes is K , then the overall latency with pipelining is $(L + K)T$ (instead of KLT without pipelining). Compared to the latency of LT for a single inference, the overhead $\frac{(L+K)T-LT}{LT} = \frac{K}{L}$ is slightly greater than 0 for large L , i.e., deeper neural networks, which is becoming widely used in practice.

If a single inference costs power P , then the power consumption of K votes would be KP , which cannot be reduced by parallel computing or pipelining. However, $P \propto V^2$, where V is the memory programming/sensing voltage, and V is positively related to SNRs, which is the inverse of σ_{val}^2 . Therefore, smaller V brings with it smaller power consumption at the cost of increasing σ_{val} . The trade-offs between power consumption and accuracy, connected by V and σ_{val} is complicated and beyond the scope of this paper.

4. Noisy Inference as a Defensive Mechanism for Black-box Adversarial Attacks

We show in this section that noisy inference can enhance adversarially trained neural networks against black-box adversarial attacks. Noisy inference provides stochastic gradients which has been shown in [27] to provide a false sense of security against white-box attacks. However, we observe that the transferability of adversarial examples from one neural network to the other has been weaker if the neural networks used for prediction have noisy inference. We focus on L_∞ attacks where all pixel values of an adversarial example are within an ϵ -cube of a natural one. Our experiments are setup as follows.

1. We use two datasets, MNIST images and CIFAR10 where all pixel values are normalized between 0 and 1.

2. The adversarial attacks are iterative fast gradient sign methods (FGSM) with projected gradient descent (PGD) and multiple restarts from a random image within the ϵ -cube of a natural image. It is shown to be a strongest attack based on first-order statistics [21]. The detailed parameters of the attacks are listed in Table 10.

	MNIST	CIFAR10
ϵ	0.3	$\frac{8}{256}$
Adv. learn. rate	0.05	$\frac{2}{256}$
Iterations	20	7
No. restarts	20	10

Table 10: Parameters of adversarial attacks (iterative FGSM).

3. Two neural networks are noiselessly ($\sigma_{\text{train}} = 0.0$) and adversarially trained [21], where each minibatch of size 32 consists of equal number of natural and adversarial samples. One neural network is used to generate adversarial examples (denoted by NN_{adv}) and the other is used to validate the accuracy of those adversarial examples (denoted by NN_{val}). For MNIST, NN_{adv} is a 4-layer CNN as it is in [21] and NN_{val} is the 6-layer CNN we presented in Table 1. Both neural networks are adversarially trained for 100 epochs. For CIFAR10, NN_{adv} is the depth-40 Densenet with growth rate 12 and NN_{val} is a depth-100 Densenet with growth rate 12. Both neural networks are adversarially trained for 300 epochs.

Table 11 shows the average validation accuracy for MNIST and CIFAR10 under black-box attacks with 20 runs of noisy inference. It can be observed that the robustness of the adversarially trained neural networks (the 6-layer CNN and the depth-100 Densenet) against the attacks has been further enhanced from 97.40% to 97.90% and from 66.52% to 67.65%, respectively. The 0.5% and 1.13% improvements are achieved by multiplicative noisy inference with $\sigma_{\text{val},x} = 0.2$ and 0.1, respectively.

5. Conclusion

In this paper, we propose to use training with injected noise and inference with voting that imbues neural networks with much greater resilience to imperfect computations during

	MNIST	CIFAR10
$\sigma_{\text{val},x} = 0.0$	97.40%	66.52%
$\sigma_{\text{val},x} = 0.1$	97.79%	67.65%
$\sigma_{\text{val},x} = 0.2$	97.90%	67.43%
$\sigma_{\text{val},x} = 0.3$	97.71%	66.57%
$\sigma_{\text{val},x} = 0.4$	97.00%	63.39%

Table 11: Accuracy of black-box attacks on MNIST and CIFAR10 for different inference noise levels $\sigma_{\text{val},x}$.

inference, which has potential applications on deep learning with ultra-low power consumptions. Three examples of neural network architectures show remarkable improvement on accuracy using these two methods. With strong noise ($\sigma_{\text{val},x} = 1$), these two methods can improve accuracy from (21.1%, 29.9%, 15.5%) to (99.5%, 89.1%, 89.6%) for the three datasets, respectively. With low-to-medium values of noise power ($\sigma_{\text{val},x} \leq 0.4$), noise-injected training itself can improve accuracy from (95.8%, 88.5%, 49.8%) to (99.4%, 91.5%, 94.3%) for the three datasets at no cost of latency or power consumption.

Further study of black-box attacks against neural networks show 0.5% and 1.13% enhancement for MNIST and CIFAR10, which is brought by noisy inference on adversarially trained neural networks.

References

- [1] J. Schmidhuber, Deep learning in neural networks: An overview, *Neural Networks* 61 (2015) 85–117, published online 2014; based on TR arXiv:1404.7828 [cs.NE]. doi:10.1016/j.neunet.2014.09.003.
- [2] T. Hastie, R. Tibshirani, J. Friedman, *The Elements of Statistical Learning*, Springer, New York, 2001.
- [3] K. Jarrett, K. Kavukcuoglu, M. Ranzato, What is the best multi-stage architecture for object recognition?, in: *IEEE Int. Conf. Computer Vision*, Kyoto, Japan, 2009, p. 21462153.
- [4] A. Krizhevsky, I. Sutskever, G. Hinton, Imagenet classification with deep convolutional neural networks, in: F. Pereira, C. J. C. Burges, L. Bottou, K. Q. Weinberger (Eds.), *Advances in Neural Information Processing Systems 25*, Curran Associates, Inc., 2012, pp. 1097–1105.
- [5] A. Graves, M. Liwicki, S. Fernandez, R. Bertolami, H. Bunke, J. Schmidhuber, A novel connectionist system for improved unconstrained handwriting recognition, *IEEE Trans. Pattern Analysis and Machine Intelligence* 31 (5) (2009) 855 – 868.
- [6] H. Sak, A. Senior, F. Beaufays, Long short-term memory recurrent neural network architectures for large scale acoustic modeling.
- [7] M. Riedmiller, H. Braun, A direct adaptive method for faster backpropagation learning: the RPROP algorithm, in: *IEEE Int. Conf. Neural Networks*, San Francisco, CA, USA, 2009, pp. 586–591.
- [8] R. Hecht-Nielsen, Theory of the backpropagation neural network, in: *Int. Joint Conf. on Neural Networks (IJCNN)*, Washington, DC, USA, 1989, pp. 593–605.
- [9] W. Zhao, G. Agnus, V. Derycke, A. Filoramo, J. Bourgoin, C. Gamrat, Nanotube devices based crossbar architecture: toward neuromorphic computing, *Nanotechnology* 21 (17).
- [10] R. Micheloni, A. Marelli, K. Eshghi, *Inside Solid State Drives (SSDs)*, Springer, New York, 2013.
- [11] B. Feinberg, S. Wang, E. Ipekn, Making memristive neural network accelerators reliable (02 2018).
- [12] S. Jain, A. Ranjan, K. Roy, A. Raghunathan, Computing in memory with spin-transfer torque magnetic ram, *IEEE Transactions on Very Large Scale Integration (VLSI) Systems* 23 (3) (2017) 470–483.
- [13] C. Szegedy, W. Zaremba, I. Sutskever, J. Bruna, D. Erhan, I. J. Goodfellow, R. Fergus, Intriguing properties of neural networks, CoRR abs/1312.6199.

- [14] I. J. Goodfellow, J. Shlens, C. Szegedy, Explaining and harnessing adversarial examples, CoRR abs/1412.6572. [arXiv:1412.6572](https://arxiv.org/abs/1412.6572).
URL <http://arxiv.org/abs/1412.6572>
- [15] A. Kurakin, I. J. Goodfellow, S. Bengio, Adversarial examples in the physical world, CoRR abs/1607.02533. [arXiv:1607.02533](https://arxiv.org/abs/1607.02533).
URL <http://arxiv.org/abs/1607.02533>
- [16] N. Carlini, D. A. Wagner, Towards evaluating the robustness of neural networks, CoRR abs/1608.04644. [arXiv:1608.04644](https://arxiv.org/abs/1608.04644).
URL <http://arxiv.org/abs/1608.04644>
- [17] N. Papernot, P. D. McDaniel, I. J. Goodfellow, Transferability in machine learning: from phenomena to black-box attacks using adversarial samples, CoRR abs/1605.07277. [arXiv:1605.07277](https://arxiv.org/abs/1605.07277).
URL <http://arxiv.org/abs/1605.07277>
- [18] N. Papernot, P. D. McDaniel, X. Wu, S. Jha, A. Swami, Distillation as a defense to adversarial perturbations against deep neural networks, CoRR abs/1511.04508. [arXiv:1511.04508](https://arxiv.org/abs/1511.04508).
URL <http://arxiv.org/abs/1511.04508>
- [19] W. Xu, D. Evans, Y. Qi, Feature squeezing: Detecting adversarial examples in deep neural networks, CoRR abs/1704.01155. [arXiv:1704.01155](https://arxiv.org/abs/1704.01155).
URL <http://arxiv.org/abs/1704.01155>
- [20] R. Feinman, R. R. Curtin, S. Shintre, A. B. Gardner, Detecting adversarial samples from artifacts, CoRR abs/1703.00410.
- [21] A. Madry, A. Makelov, L. Schmidt, D. Tsipras, A. Vladu, Towards deep learning models resistant to adversarial attacks, in: International Conference on Learning Representations, 2018.
URL <https://openreview.net/forum?id=rJzIBfZAb>
- [22] G. Huang, Z. Liu, K. Q. Weinberger, Densely connected convolutional networks, CoRR abs/1608.06993. [arXiv:1608.06993](https://arxiv.org/abs/1608.06993).
URL <http://arxiv.org/abs/1608.06993>
- [23] E. D. de Jong, Mnist digits stroke sequence data, <https://github.com/edwin-de-jong/mnist-digits-stroke-sequence-data/wiki/MNIST-digits-stroke-sequence-data> (2016).
- [24] R. Hahnloser, R. Sarpeshkar, M. Mahowald, R. J. Douglas, H. S. Seung, Digital selection and analogue amplification coexist in a cortex-inspired silicon circuit, *Nature* (405) (2000) 947951.
- [25] A. L. Maas, A. Y. Hannun, A. Y. Ng., Rectifier nonlinearities improve neural network acoustic models (2013).
- [26] K. He, X. Zhang, S. Ren, J. Sun, Deep residual learning for image recognition, CoRR abs/1512.03385. [arXiv:1512.03385](https://arxiv.org/abs/1512.03385).
URL <http://arxiv.org/abs/1512.03385>
- [27] A. Athalye, N. Carlini, D. A. Wagner, Obfuscated gradients give a false sense of security: Circumventing defenses to adversarial examples, CoRR abs/1802.00420. [arXiv:1802.00420](https://arxiv.org/abs/1802.00420).
URL <http://arxiv.org/abs/1802.00420>